ChemComm

Accepted Manuscript

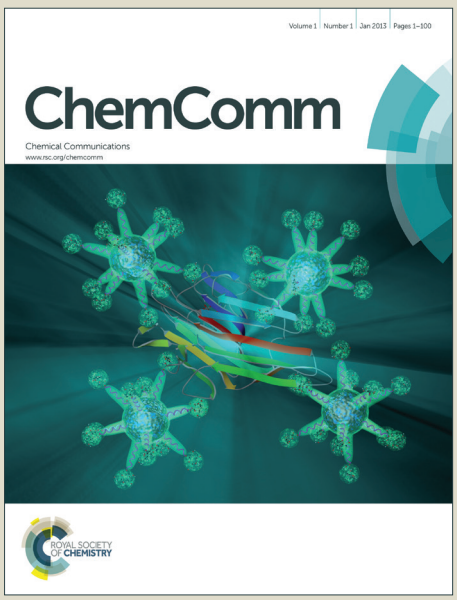

ROYAL SOCIETY OF CHEMISTRY

www.rsc.org/chemcomm

Journal Name

RSCPublishing

COMMUNICATION

Dye-sensitized Pt@UiO-66(Zr) metal-organic framework for visible-light photocatalytic hydrogen production

Jiao He, Jiaqiang Wang,* Yongjuan Chen, Jinping Zhang, Deliang Duan, Yao Wang and Zhiying Yan*

Cite this: DOI: 10.1039/x0xx00000x

Received 00th January 2012,
Accepted 00th January 2012

DOI: 10.1039/x0xx00000x

www.rsc.org/

A stable photoactive metal-organic framework UiO-66(Zr) sensitized by adsorbed or directly added Rhodamine B dye exhibited photocatalytic activity for hydrogen evolution under visible-light illumination (λ≥420nm). Pt as a co-catalyst, the adsorbed and directly added dye extremely enhanced the photocatalytic activity to 30 and 26 times of the value afforded by bare Pt@UiO-66(Zr), respectively.

In search of solutions to the increasingly serious energy and environmental problems all over the world, considerable efforts have been invested in heterogeneous photocatalytic hydrogen production based on semiconductor by water splitting. Meanwhile, metal-organic frameworks (MOFs) have aroused widespread interest recently due to their high surface areas, crystalline open structures, tunable pore size and functionality. Especially, they have a high volume fraction of active metal sites which inspired their potential applications in catalysis.[1] Although there are still some limitations, the opportunities of MOFs as heterogeneous catalysis are very encouraging.[2] Because of the well-defined crystal structures of MOFs and controllable chromophore distances via crystal engineering, highly crystalline MOFs have provided an ideal platform for designing molecular solids for light harvesting.[3]

Recently, the possibility of using MOFs as semiconductors in where photon absorption produces a state of charge separation has been explored especially on Zn-based MOF-5.[4] Even directly photocatalytic water splitting over Zr-based MOFs formed by terephthalate and 2-aminoterephthalate ligands (UiO-66 and NH_2-UiO-66) has been reported.[5] Bimetallic MOFs encapsulating infinite linear polyiodide chains also exhibited photocatalytic hydrogen production activity under UV irradiation.[6] However, these MOFs are not highly effective for photocatalysis and one of the reasons could be that they cannot respond to visible-light effectively.

There are mainly two approaches to obtain visible-light responsive MOFs. One is to select ligands or metal centres with visible-light response and the other is post-synthetically functionalization. For example, porphyrins are versatile functional molecules for light harvesting so a porphorin-based Al-MOF[7] and Pt nanaoparticles coated by photoactive Zr-MOF built from $[Ir(ppy)_2(bpy)]^+$-derived ligand[8] was synthesized for visible-light photocatalysis. A Fe-based MOF shows visible-light photocatalytic activity because Fe(III) oxides could be promising visible-light photocatalysts.[9] An amine-functionalized MIL-125(Ti)[10] and UiO-66(Zr)[11] exhibited photocatalytic activities under visible-light for CO_2 reduction. The NH_2-MIL-125(Ti) can also be used to produce hydrogen by using Pt cocatalyst[12] while the NH_2-UiO-66(Zr) could degrade organic dyes under visible-light.[13] Recently, even the amino group of the NH_2-MIL-125(Ti) has been post-functionalized with dye-like molecular fragment to improve its visible-light activity.[14] Besides, photocatalytic hydrogen generation over a Ru-MOF with $Ru(bpy)_3^{2+}$ as photosensitizer, MV^{2+} (N,N'-dimethyl-4,4'-bipyridinium) as an electron relay and EDTA-2Na as electron donor has been realized.[15] The Cu-doped ZIF-67(Co) could also be used for visible-light photocatalysis.[16]

Meanwhile, it must be mentioned that since dye-sensitized colloidal TiO_2 films with enhanced light-to-electric energy conversion yield was reported in 1991,[17] dye-sensitization has become a relatively mature technology for visible-light harvesting when it comes to semiconductor photocatalysts. Given the aforementioned photoactivities of MOFs, one may wondered if a dye-sensitized photocatalytic process in a MOF could be accomplished. Integrating the concept of dye-sensitized semiconductor into MOF-based photocatalyst may adopt the merits of both MOF and semiconductor to overcome their respective drawback for photocatalysis.

We have reported in our previous work that the sensitization of CdS by visible-light responsive MIL-101(Cr) could beneficial to photocatalytic hydrogen production over CdS.[18] In this work, UiO-66(Zr) was considered as photocatalyst for hydrogen production due to its intrinsic photoactivity[5] and good thermal stability.[19] UiO-66(Zr) was prepared by using a modified procedure as described in literature.[5] Pt nanoparticles (NPs) were then incorporated and Rhodamine B (RhB) dye was used as sensitizer to absorb visible-light. The X-ray diffraction

(XRD) pattern (see Fig. S1 in the ESI), a type I nitrogen adsorption/desorption isotherm (Fig. S2) and a Langmuir surface area of ~1026.0 m^2/g confirm that UiO-66(Zr) was properly synthesized. As shown in Fig. 1a, the synthesized UiO-66(Zr) composed of cubes in the scale of 30 to 50 nm. Pt was introduced into UiO-66(Zr) by reduction of H_2PtCl_6 with ascorbic acid. HR-TEM (Fig. 1b) revealed that Pt NPs obtained with a particle size distribution of about 3 to 5 nm disperse over the UiO-66(Zr). This confirmed the successful preparation of Pt@UiO-66(Zr).

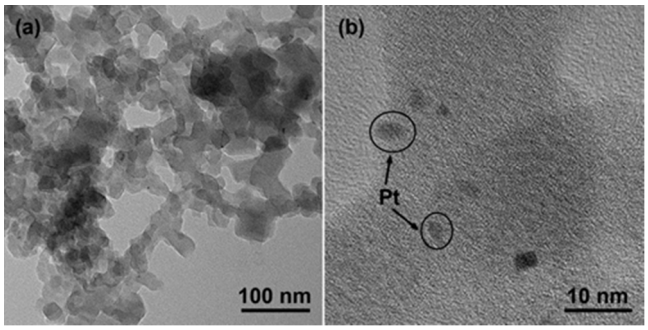

Fig. 1 (a) TEM image of UiO-66(Zr) and (b) HR-TEM of Pt@UiO-66(Zr) showing Pt NPs.

Pure UiO-66(Zr) is white powder with barely absorption in the visible-light region (λ≥420nm). UV-vis diffraction spectrum (DRS) (Fig. 2) shows that UiO-66(Zr) has an absorption band-edge of 335 nm. The absorption in UV region could be attributed to the π→π* transition in organic ligands. It has been reported that UiO-66(Zr) possesses photocatalytic activity because of its ability to act like semiconductors.[5] Effective photoexcitation leads to charge separation with electrons populating the lowest unoccupied molecular orbital (LUMO) and holes in the highest occupied molecular orbital (HOMO).[5] Based on the relation E_g=1240/λ, the calculated band gap of UiO-66(Zr) is 3.05 eV. Meanwhile, it is worth noting the viewpoint that MOFs should be seen as an array of self-assembled molecular catalysts rather than as classical semiconductors and the optical absorption spectra depicted of them should be considered as sets of individual discrete absorption bands. So the HOMO-LUMO gap terminology should be used in order to describe the discrete characteristics of the light-induced transitions in these coordination compounds.[14] The introduction of Pt NPs contributes to the enhancement of light absorption intensity of the UiO-66(Zr) in the visible-light region, which is in accordance with the colour change of the samples, from white to pale grey. When RhB was adsorbed, the sample turned into purplish pink. UV-vis DRS shows that the absorption intensity of Pt@UiO-66(Zr) in visible-light region was greatly improved after being sensitized by RhB and the absorption range was expanded to about 600 nm. The result suggests potential photocatalytic activity of the RhB-sensitized Pt@UiO-66(Zr) under visible-light irradiation. In comparison with RhB aqueous solution, the DRS of RhB adsorbed on UiO-66(Zr) in the visible-light region was not significantly changed and the location of intrinsic absorption peak is still about 554 nm. This implies that the structures of the dye molecules were not changed and there are no strong interactions between RhB dye and the MOFs.

Mott-Schottky plots of UiO-66(Zr) were measured at frequency of 1000 and 1500 Hz. As shown in Fig. 3, the positive slope of the obtained C^{-2} to Potemtial plot is consistent with that of typical n-type semiconductors. The intersection points do not depend on the different frequency applied. The flat band position (V_{fb}) determined from the intersection is approximately -0.70 V *vs*. Ag/AgCl (i.e. -0.50 V *vs*. NHE) for UiO-66(Zr). Since it is generally believed that the bottom of the conduction band in many n-type semiconductors is more negative by about 0.10 V than the flat band potential,[20] the conduction band (LUMO) of UiO-66(Zr) can be estimated to be -0.60 V *vs*. NHE, which is more negative than the redox potential of H^+/H_2 (-0.41 V *vs*. NHE, pH=7).[21] According to a band gap of 3.05 eV as described above, the valence band (HOMO) can be calculated to be 2.45 V *vs*. NHE.

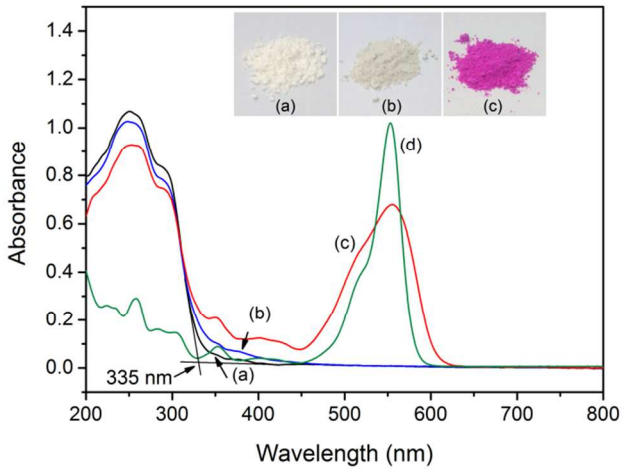

Fig. 2 UV-vis diffraction spectra of (a) UiO-66(Zr), (b) Pt@UiO-66(Zr), (c) RhB-sensitized Pt@UiO-66(Zr) and (d) 5 ppm RhB aqueous solution (inset shows photographs of a, b and c).

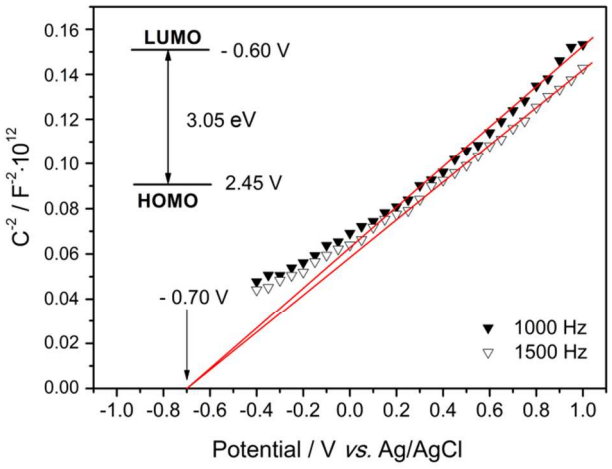

Fig. 3 Mott–Schottky plot of UiO-66(Zr) in 0.2 M Na_2SO_4 aqueous solution.

In a dye-sensitized photocatalytic system, dyes absorb visible-light to form electronically excited states. The redox potentials of RhB and excited RhB* are 0.95 V and -1.42 V *vs*. NHE, respectively.[22] Considering the potential of LUMO in UiO-66(Zr) (-0.60 V *vs*. NHE),

direct electron transfer from RhB* to UiO-66(Zr) is thermodynamically favourable. Therefore, it is permissible for the reduction of protons to realize photocatalytic H_2 generation.

The photocatalytic activities of the catalysts were evaluated in the presence of triethanolamine (TEOA) as an electron donor. As shown in Fig. 4a, although photocatalytic H_2 production over UiO-66(Zr) irradiated by a xenon-doped mercury lamp has been reported,[5] no appreciable H_2 evolution was detected over pure UiO-66(Zr) under visible-light irradiation in this work. This is because UiO-66(Zr) is not able to absorb and utilize visible-light. But when 1 wt % of Pt NPs are incorporated, the Pt@UiO-66(Zr) shows an rate of 3.9 μmol/g·h for H_2 production (Fig. 4b). This is consistent with the slightly enhancement on light absorption intensity of Pt@UiO-66(Zr) in the visible-light region (Fig. 2).

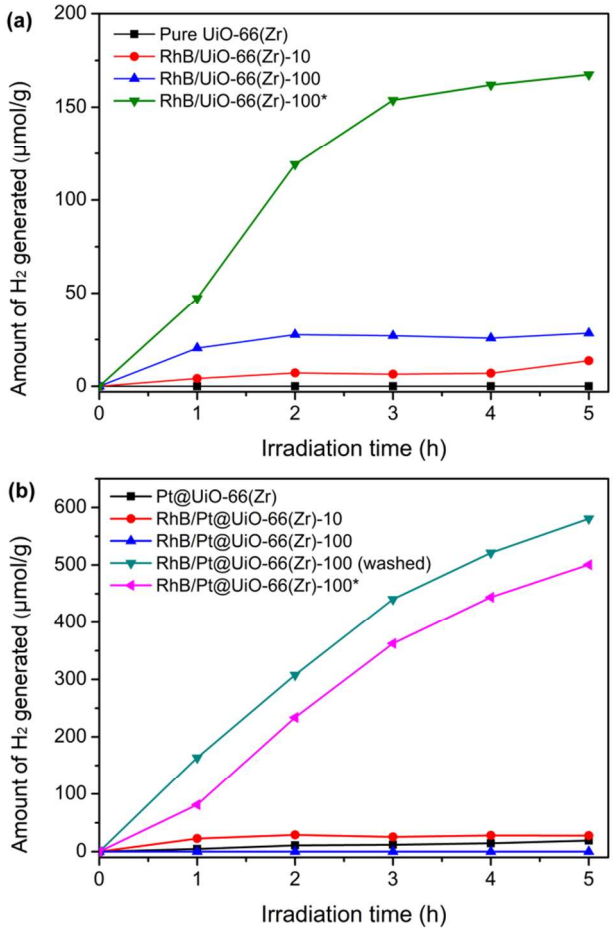

Fig. 4 Photocatalytic H_2 production over (a) UiO-66(Zr), RhB-sensitized UiO-66(Zr), (b) Pt@UiO-66(Zr) and RhB-sensitized Pt@UiO-66(Zr) under visible-light.

The UiO-66(Zr) and Pt@UiO-66(Zr) were sensitized by using 10ppm and 100ppm RhB ethanol solution (denoted as RhB/UiO-66(Zr)-X and RhB/Pt@UiO-66(Zr)-X, X=10, 100). As shown in Fig. 4a and Table S2, RhB/UiO-66(Zr)-10 (1.63mg/g RhB adsorbed) exhibited a photocatalytic activity of 2.7 μmol/g·h. However, when more dyes were adsorbed on UiO-66(Zr) (7.43 mg/g for RhB/UiO-66(Zr)-100), the H_2 generation rate was not significantly increased as expected. But when the same amount of dye adsorbed on RhB/UiO-66(Zr)-100 (7.43 mg/g) was directly added into the solution just before light irradiation (RhB/UiO-66(Zr)-100* in Fig. 4a), the photocatalytic activity reached 33.9μmol/g·h. The results show that RhB in solution can also sensitize UiO-66(Zr) effectively. And more importantly, the dosage of dye had a great influence on the photocatalytic activity.

When Pt was used as a co-catalyst, as shown in Fig. 4b, RhB/Pt@UiO-66(Zr)-10 (2.54 mg/g of RhB adsorbed) exhibited a low photocatalytic activity of 5.6 μmol/g·h while no significant H_2 was generated over RhB/Pt@UiO-66(Zr)-100 (11.92 mg/g of RhB adsorbed). Very interestingly, the washed RhB/Pt@UiO-66(Zr)-100, which lost some of the excessive adsorbed dyes, exhibited the highest photocatalytic activity of 116.0 μmol/g·h, which is thirty-fold greater than that of bare Pt@UiO-66(Zr). Moreover, the same dosage of RhB adsorbed on RhB/Pt@UiO-66(Zr)-100 (11.92 mg/g) could also give a high activity when the dye was directly added (RhB/Pt@UiO-66(Zr)-100* in Fig. 4b), which is 26-fold greater than that of bare Pt@UiO-66(Zr). Therefore, the photocatlytic activities of both UiO-66(Zr) and Pt@UiO-66(Zr) were not positively correlated to the amounts of dye adsorbed. Directly adding the dye to the solution can also receive a high H_2 production rate in comparison to adsorbing dye previously. We propose that when too much dye was adsorbed on the catalyst, the excessive dye molecules might block the spread of incident light and effective electron transport to depress the photocatalytic H_2 production. On the other hand, Pt@UiO-66(Zr) exhibited much higher photocatalytic activity than pure UiO-66(Zr) in this dye-sensitization process, suggesting the efficient charge separation caused by the presence of Pt NPs as cocatalyst[12b] and the low overpotential for H_2 evolution at Pt surface. In this particular instance, Pt NPs introduce active sites required for efficient H_2 evolution in combination with the light absorbing unit, RhB.

The adsorbed RhB dye is easy to be desorbed and diffuse into the solution. As a result, the stability of the dye sensitizer is not good. But the XRD patterns of the fresh and used RhB-sensitized Pt@UiO-66(Zr) (Fig. S4) are almost the same, implying that Pt@UiO-66(Zr) is resistant for light irradiation. The photostability of Pt@UiO-66(Zr) was also investigated over three runs of totally 15 h (Fig. S5). Therefore, the further research should concern to the stability of dye sensitizer by restraining adsorbed dye molecules.

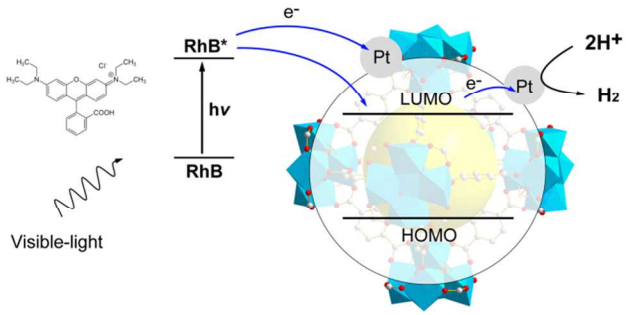

Fig. 5 Proposed mechanism of photocatalytic H_2 production over RhB-sensitized Pt@UiO-66(Zr) under visible-light.

A probable mechanism for photocatalytic hydrogen production process mentioned has been proposed as follow (Fig. 5): When the RhB

molecules are directly adsorbed on Pt@UiO-66(Zr) and excited under visible-light irradiation, a large energy band offset will form between RhB^* and UiO-66(Zr), and then the excited electrons will most likely transfer to the LUMO of UiO-66(Zr) composed by empty metal orbitals. When Pt NPs were deposited on UiO-66(Zr), a Schottky barrier can form at the interface of UiO-66(Zr) and Pt NPs due to the higher work function of Pt than UiO-66(Zr). Therefore, the trapped electrons in the UiO-66(Zr) matrix could subsequently transfer to Pt nanoparticles, which spatially separated $RhB^{\bullet+}$ and electrons, thus restraining the recombination process and promoting electron transfer and photocatalytic reactions for hydrogen evolution. Besides, the excited RhB^* can also inject electrons directly to the Pt to produce H_2. Meanwhile, the generated $RhB^{\bullet+}$ recovered to ground state by getting electrons from triethanolamine and the triethanolamine is indispensable here as an electron donor.

In summary, Pt nanoparticles were introduced into the UiO-66(Zr), which exhibited practical photocatalytic activity. The as-synthesized Pt@UiO-66(Zr) could not utilize visible-light effectively and showed very low photocatalytic H_2 production activity. However, its efficiency could be significantly enhanced by adsorbing dyes on it or directly adding dyes into the solution as it often does when it comes to a semiconductor photocatalyst. Although the H_2 generation rate in dye-photosensitized MOFs is much lower in comparison to traditional semiconductors, we believe that the simple strategy demonstrated here could be extended to other MOFs and other dyes. This could open up new uses for MOFs in applications such as dye-sensitized solar cells, or other regions considering the large variety of structures and the combination of metals and linkers.

The authors thank the National Natural Science Foundation of China (Project NSFC-YN U1033603, 21063016) and the Program for Innovative Research Teams (in Science and Technology) in the University of Yunnan Province (IRTSTYN) for financial support.

Notes and references

The Universities' Center for Photocatalytic Treatment of Pollutants in Yunnan Province, School of Chemical Science & Engineering, Yunnan University, Kunming 650091, P. R. China. E-mail: jqwang@ynu.edu.cn, zhyyan@ynu.edu.cn; Fax: +86 871 65031567; Tel: +86 871 65031567.

† Electronic Supplementary Information (ESI) available: [Details of preparation, characterizations of the photocatalysts and methods of photocatalytic hydrogen production]. See DOI: 10.1039/c000000x/

1. (a) M. Ranocchiari and J. A. van Bokhoven, *Phys Chem Chem Phys*, 2011, **13**, 6388-6396; (b) A. Dhakshinamoorthy, M. Alvaro and H. Garcia, *Chem. Commun.*, 2012, **48**, 11275-11288; (c) J. Lee, O. K. Farha, J. Roberts, K. A. Scheidt, S. T. Nguyen and J. T. Hupp, *Chem. Soc. Rev.*, 2009, **38**, 1450-1459; (d) D. Farrusseng, S. Aguado and C. Pinel, *Angew. Chem. Int. Ed.*, 2009, **48**, 7502-7513; (e) A. Corma, H. Garcia and F. X. Llabres i Xamena, *Chem. Rev.*, 2010, **110**, 4606-4655.
2. J. Gascon, A. Corma, F. Kapteijn and F. X. Llabrés i Xamena, *ACS Catalysis*, 2014, **4**, 361-378.
3. (a) C. G. Silva, A. Corma and H. García, *J. Mater. Chem.*, 2010, **20**, 3141; (b) J.-L. Wang, C. Wang and W. Lin, *ACS Catalysis*, 2012, **2**, 2630-2640; (c) C. H. Hendon, D. Tiana and A. Walsh, *Phys Chem Chem Phys*, 2012, **14**, 13120-13132; (d) Y. Horiuchi, T. Toyao, M. Takeuchi, M. Matsuoka and M. Anpo, *Phys Chem Chem Phys*, 2013, **15**, 13243-13253.
4. (a) S. Bordiga, C. Lamberti, G. Ricchiardi, L. Regli, F. Bonino, A. Damin, K. P. Lillerud, M. Bjorgen and A. Zecchina, *Chem. Commun.*, 2004, 2300-2301; (b) M. Alvaro, E. Carbonell, B. Ferrer, F. X. Llabres i Xamena and H. Garcia, *Chem-eur. J.*, 2007, **13**, 5106-5112; (c) F. X. LlabresiXamena, A. Corma and H. Garcia, *J. Phys. Chem. C*, 2007, **111**, 80-85; (d) T. Tachikawa, J. R. Choi, M. Fujitsuka and T. Majima, *J. Phys. Chem. C*, 2008, **112**, 14090-14101; (e) H. Khajavi, J. Gascon, J. M. Schins, L. D. Siebbeles and F. Kapteijn, *J. Phys. Chem. C*, 2011, **115**, 12487-12493.
5. C. Gomes Silva, I. Luz, F. X. Llabres i Xamena, A. Corma and H. Garcia, *Chem-eur. J.*, 2010, **16**, 11133-11138.
6. X. L. Hu, C. Y. Sun, C. Qin, X. L. Wang, H. N. Wang, E. L. Zhou, W. E. Li and Z. M. Su, *Chem. Commun.*, 2013, **49**, 3564-3566.
7. T. Zhou, Y. Du, A. Borgna, J. Hong, Y. Wang, J. Han, W. Zhang and R. Xu, *Energy Environ. Sci.*, 2013, **6**, 3229.
8. C. Wang, K. E. deKrafft and W. Lin, *J. Am. Chem. Soc.*, 2012, **134**, 7211-7214.
9. K. G. Laurier, F. Vermoortele, R. Ameloot, D. E. De Vos, J. Hofkens and M. B. Roeffaers, *J. Am. Chem. Soc.*, 2013, **135**, 14488-14491.
10. Y. Fu, D. Sun, Y. Chen, R. Huang, Z. Ding, X. Fu and Z. Li, *Angew. Chem. Int. Ed.*, 2012, **51**, 3364-3367.
11. D. Sun, Y. Fu, W. Liu, L. Ye, D. Wang, L. Yang, X. Fu and Z. Li, *Chem-eur. J.*, 2013, **19**, 14279-14285.
12. (a) T. Toyao, M. Saito, Y. Horiuchi, K. Mochizuki, M. Iwata, H. Higashimura and M. Matsuoka, *Catal. Sci. Technol.*, 2013, **3**, 2092; (b) Y. Horiuchi, T. Toyao, M. Saito, K. Mochizuki, M. Iwata, H. Higashimura, M. Anpo and M. Matsuoka, *J. Phys. Chem. C*, 2012, **116**, 20848-20853.
13. L. Shen, W. Wu, R. Liang, R. Lin and L. Wu, *Nanoscale*, 2013, **5**, 9374-9382.
14. M. A. Nasalevich, M. G. Goesten, T. J. Savenije, F. Kapteijn and J. Gascon, *Chem. Commun.*, 2013, **49**, 10575-10577.
15. Y. Kataoka, K. Sato, Y. Miyazaki, K. Masuda, H. Tanaka, S. Naito and W. Mori, *Energy Environ. Sci.*, 2009, **2**, 397.
16. H. Yang, X.-W. He, F. Wang, Y. Kang and J. Zhang, *J. Mater. Chem.*, 2012, **22**, 21849.
17. B. O'Regan and M. Grätzel, *Nature*, 1991, **353**, 737-740.
18. J. He, Z. Yan, J. Wang, J. Xie, L. Jiang, Y. Shi, F. Yuan, F. Yu and Y. Sun, *Chem. Commun.*, 2013, **49**, 6761-6763.
19. (a) J. H. Cavka, S. Jakobsen, U. Olsbye, N. Guillou, C. Lamberti, S. Bordiga and K. P. Lillerud, *J. Am. Chem. Soc.*, 2008, **130**, 13850-13851; (b) L. Valenzano, B. Civalleri, S. Chavan, S. Bordiga, M. H. Nilsen, S. Jakobsen, K. P. Lillerud and C. Lamberti, *Chem. Mater.*, 2011, **23**, 1700-1718.
20. (a) J. Long, S. Wang, Z. Ding, S. Wang, Y. Zhou, L. Huang and X. Wang, *Chem. Commun.*, 2012, **48**, 11656-11658; (b) L. Shen, S. Liang, W. Wu, R. Liang and L. Wu, *Dalton Trans.*, 2013, **42**, 13649-13657.
21. (a) X. Chen, S. Shen, L. Guo and S. S. Mao, *Chem. Rev.*, 2010, **110**, 6503-6570; (b) Y. Xu and M. A. Schoonen, *Am. Mineral.*, 2000, **85**, 543-556.
22. Z. Xiong, L. L. Zhang, J. Ma and X. S. Zhao, *Chem. Commun.*, 2010, **46**, 6099-6101.

Supporting Information

for

Dye-sensitized Pt@UiO-66(Zr) metal-organic framework for visible-light photocatalytic hydrogen production

Jiao He, Jiaqiang Wang,* Yongjuan Chen, Jinping Zhang, Deliang Duan, Yao Wang, Zhiying Yan*

The Universities' Center for Photocatalytic Treatment of Pollutants in Yunnan Province, School of Chemical Sciences & Engineering, Yunnan University, Kunming 650091, People's Republic of China.

Tel.: +86 871 65031567, Fax: +86 871 65031567

E-mail: jqwang@ynu.edu.cn (J. Wang)

Preparation of photocatalysts

UiO-66: UiO-66 was prepared following a modified procedure as described in literature [1]. In a typical synthetic process, 106 mg of $ZrCl_4$ and 68 mg of 1,4-benzenedicarboxylic acid were dissolved in 50 mL dimethyl formamide (DMF) and sealed in a stainless steel vessel with Teflon liner. The solution was then put into a preheated oven at 120 ^oC. After 48 h, the oven was naturally cooled to room temperature. The solid was filtered out, washed with DMF and absolute ethyl alcohol and then dried in air at 90 ^oC.

Pt@UiO-66: 1 wt % Pt nanoparticles were introduced to UiO-66. 1 g of UiO-66 was dispersed in 100 mL aqueous solution containing a certain amount of H_2PtCl_6 and stirring for 6 h. After that, ascorbic acid was added following by another 6 h for stirring. The solid was filtered out, washed and dried in air at 90 ^oC.

Characterizations

Wide angle X-ray powder diffraction (XRD) experiments were conducted on a Rigaku TTRAX III spectrometer with Cu Kα radiation from 3^o to 80^o. Nitrogen adsorption/desorption measurements were carried out on a Micromeritics Tristar II Suaface area and porosity analyzer. HR-TEM micrographs were obtained using a JEM-2100 microscope. UV-Vis diffuse reflectance spectra were measured on a Shimadzu UV-2401PC photometer from 200 nm to 800 nm. The Mott-Schottky curves were measured using a ZENNIUM electrochemical analyzer (Germany) in a three-electrode cell. Pt plate was used as counter electrode and Ag/AgCl electrode

(3M KCl) was used as reference electrode. The electrolyte was a 0.2 M Na_2SO_4 solution. The working electrode was prepared on fluorine-doped tin oxide (FTO) glass by dipping the mixed slurry containing the sample and H_2O on it, and the exposed area of the electrode was 0.25 cm^2.

Photocatalytic hydrogen production

The catalysts were sensitized in two different ways: (i) prior to photocatalytic reaction, the catalysts was sensitized by adsorption of organic dye before photocatalytic reaction. The catalysts were dispersed in 100 ppm Rhodamin B (RhB) ethanol solution for 48 h. The pink solids were filtered out, washed several times with ethanol until the eluant was observed no colors and dried in air at 90 ^oC. The concentrations of RhB solutions before and after use were determined by UV-Vis spectrum at wavelength 554 nm and to calculate the adsorbing capacities of the catalysts. (ii) The dyes were adsorbed in situ. Specific amount of dye was added into the solution before the light irradiation.

The photocatalytic hydrogen evolution by water splitting was performed in a glass reaction cell with quartz cover connected to a closed gas circulation and the gas circulation was swept by high purity N_2 before illumination. 50 mg photocatalyst was dispersed in 100 mL of 10 vol % triethanolamine (TEOA) aqueous solution (pH=7.0). Then the suspension was exposed to a 300 W Xe lamp equipped with an optical filter (λ>420nm) to cut off the light in the ultraviolet region. The reaction solution was stirred continuously and cooled to room temperature by a circulation of cooling water.

The amount of hydrogen evolved was determined at an interval of 1 h with online gas chromatography.

[1] C. Gomes Silva, et al. *Chemistry-A European Journal.* 2010, 16(36): 11133-11138.

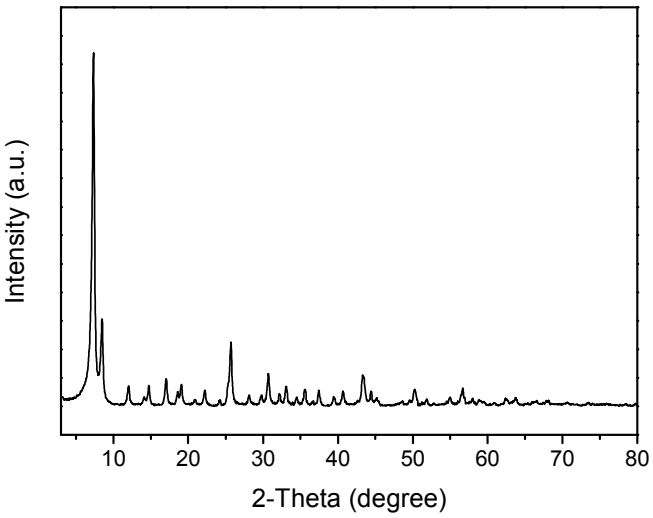

Figure S1. Wide-angle XRD pattern of UiO-66(Zr).

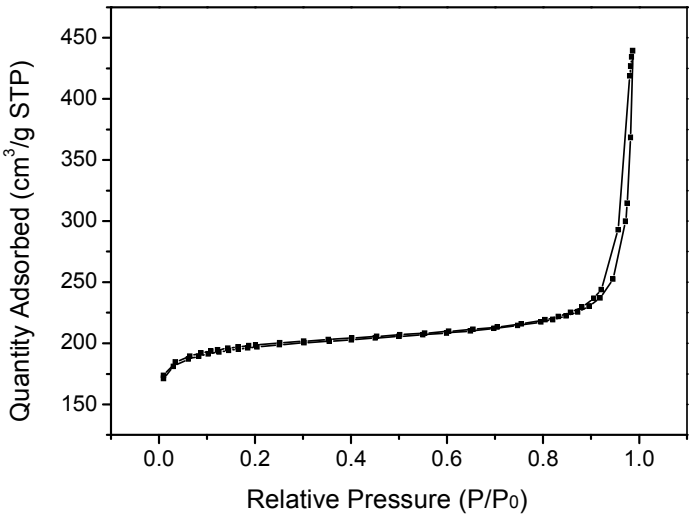

Figure S2. N_2 adsorption/desorption isotherm of UiO-66(Zr).

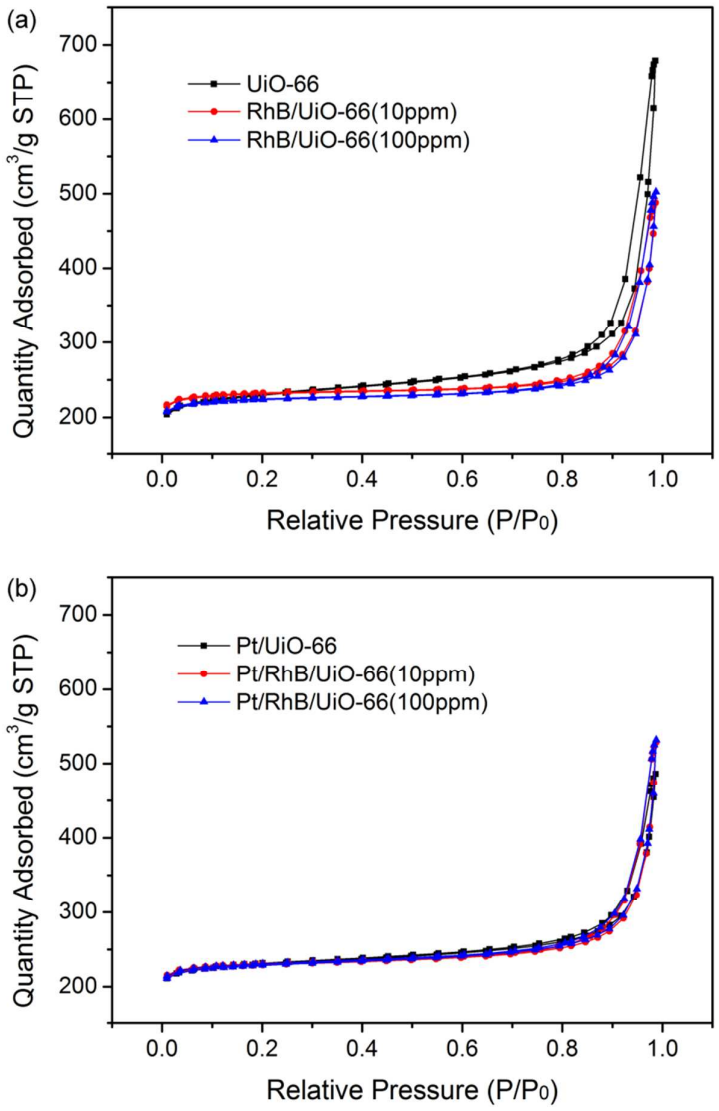

Figure S3. N_2 adsorption/desorption isotherm of (a) UiO-66(Zr) and RhB-sensitized UiO-66(Zr) by using RhB solutions with different concentration,

(b) Pt-loaded UiO-66(Zr) and RhB-sensitized Pt/UiO-66(Zr).

Table S1. Surface areas of the as-synthesized catalysts.

Catalyst	Langmuir surface area (m^2/g)	Dye adsorbed (mg/g)
UiO-66(Zr)	1025.96	-
RhB/UiO-66(Zr)-10	1019.47	1.63
RhB/ UiO-66(Zr)-100	986.18	7.43
Pt@UiO-66(Zr)	1016.99	-
RhB/Pt@UiO-66(Zr)-10	1010.03	2.54
RhB/Pt@UiO-66(Zr)-100	1009.74	11.92

Table S2. H_2 production rate of the catalysts.

Catalyst	Amount of RhB added (mg/g_{cat})	H_2 production rate (μmol/g·h)
UiO-66(Zr)	-	0
	1.63 (adsorbed)	2.7
	7.43 (adsorbed)	5.7
	7.43 (directly added)	33.9
Pt@UiO-66(Zr) (1 wt%)	-	3.9
	2.54 (adsorbed)	5.6
	11.92 (adsorbed)	0
	11.92 (adsorbed washed)	116.1
	11.92 (directly added)	100.1

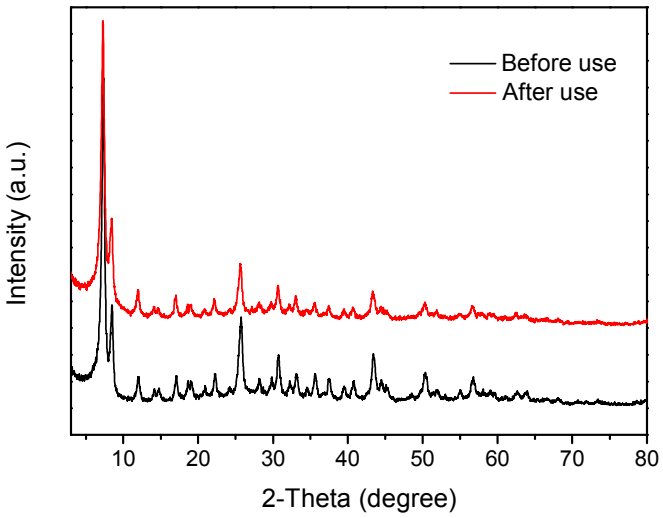

Figure S4. XRD patterns of RhB-sensitized Pt@UiO-66(Zr) (before and after use).

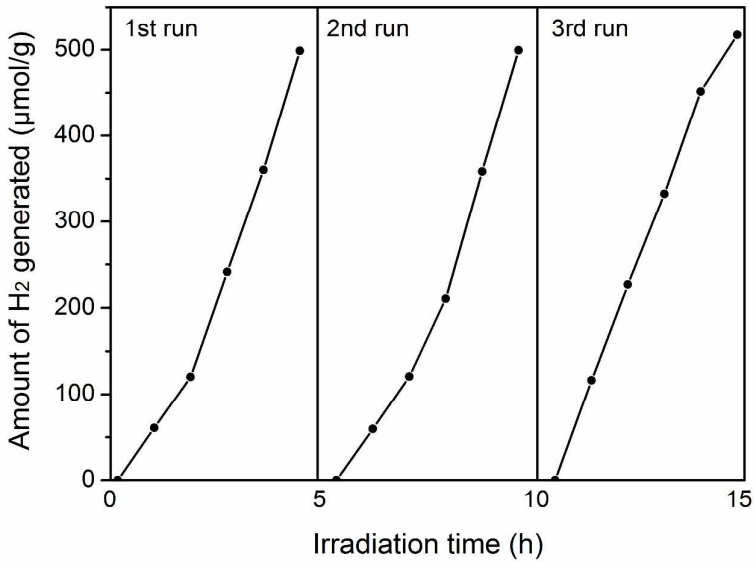

Figure S5. Time course of H_2 production over RhB-sensitized Pt@UiO-66(Zr) under visible-light.

Reaction condition: 300W Xe lamp with UV cut filter (λ>420nm) was used as the light source, 100 mL of 10 vol % triethanolamine (TEOA) aqueous solution (pH=7.0) as electron donor. 50 mg of Pt@UiO-66(Zr) was used and the RhB was added into the solution before the light reaction (11.92 mg/g). After the reaction, the catalyst was washed, filtered out and reused.